TUDelft

Delft University of Technology

Closed-Form Analysis of Artificial Dielectric Layers with Non-Periodic Characteristics

Cavallo, Daniele; van Schelven, Ralph M.

Important note
To cite this publication, please use the final published version (if applicable).
Please check the document version above.

Closed-Form Analysis of Artificial Dielectric Layers with Non-Periodic Characteristics

Daniele Cavallo[1] and Ralph M. van Schelven[1]

[1] Microelectronics Department, Delft University of Technology, Delft, The Netherlands, d.cavallo@tudelft.nl

Abstract—We present a general analysis to describe non-periodic artificial dielectric layers (ADLs). Closed-form expressions for the equivalent layer impedance are given for generic plane-wave incidence, assuming that each individual layer can differ from the others in terms of geometrical parameters. By dropping the assumption of identical layers, the given formulas are of more general applicability for flexible designs artificial dielectric slabs that are not uniform along the stratification. The analytical expressions account for the interaction between layers due to higher-order Floquet modes, thus remain valid for arbitrarily small electrical distance between layers.

Index Terms—Artificial dielectric layers, closed-form solutions, equivalent circuit.

I. INTRODUCTION

An artificial dielectric (AD) consists of a periodic arrangement of metallic inclusions in a hosting medium to realize a material with higher effective refractive index [1], [2]. The equivalent electromagnetic parameters of the AD can be engineered by properly designing the density and the shape of the metallic objects. Both the size of the metal objects and the periods of the three dimensional lattice are much smaller compared to the wavelength. In this way, the metallic scatterers play the same roles of atoms or molecules in a real dielectric, by producing a net average polarization field that opposes the external electric field, giving rise to an effective permittivity [3].

This work deals with a specific type of anisotropic AD, where the metallic objects are sub-wavelength planar patches, as shown in Fig. 1. Such structures are referred to as artificial dielectric layers (ADLs). Recently, ADLs were exploited to improve the front-to-back ratio of integrated antennas at mm-wave frequencies [4], [5]. The main advantage of an ADLs compared to a real dielectric is the anisotropy, which is a key property to avoid the excitation of surface waves. Another application was proposed in [6], [7], where the ADLs were used in combination with planar connected arrays to achieve wideband and wide angle scanning phased array designs. The anisotropy of the ADLs allows enlarging the scan range with no scan blindness, while performing a wideband impedance transformation, to widen the impedance matching bandwidth.

For the electromagnetic modeling of ADLs, a number of numerical solutions proposed for the efficient analysis of generic multilayer metasurfaces can be used, for example [8]–[10]. More recently, analytical formulas to describe ADLs were presented in [11], [12] for aligned layers (Fig. 1(a)) and generalized in [13] to include a shift between even and odd
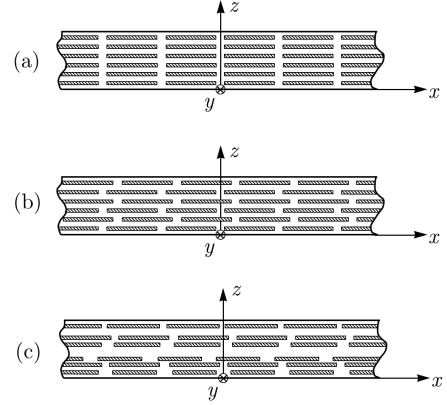

Fig. 1. Two-dimensional side view for artificial dielectric slabs with (a) aligned, (b) shifted and (c) non-periodic layers along z.

layers (Fig. 1(b)). An extension of the method to include the finite conductivity of the metal was presented in [14]. All the mentioned works provide a transmission line model to represent the propagation of a generic plane wave within the ADLs. In such equivalent circuit, each layer is represented as an equivalent shunt impedance, which can be expressed in closed-form as a function of the geometrical parameters of the ADLs. Compared to other works with similar scope [16]–[18], the equivalent impedances in [13], [14] include the reactive coupling between layers due to higher-order Floquet modes. Given the very small electrical distance between layers in typical ADL designs, such coupling is very large and must be taken into account.

The previous works [12]–[14] only contemplated z-periodic structures, where the layers of patches are all identical, aligned as in Fig. 1(a) or alternatively shifted to realize a glide symmetric structure [15] as in Fig. 1(b). In this work, we propose a technique to generalize the method to deal with non-periodic structure, as the one depicted in Fig. 1(c). The structure is still doubly periodic in the x-y plane, but each layer along the z-axis can have different geometrical parameters, namely the gaps between patches, the distance and the shift to the layer above or below. The closed-form expressions given here can be used to design more complex non-uniform ADLs that can provide a variation of effective permittivity along the direction of stratification z.
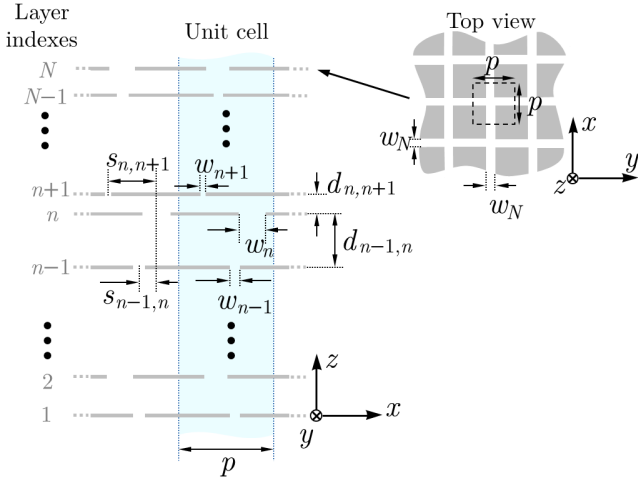
Fig. 2. Cross section view of the unit cell of z-aperiodic ADLs, with definition of the geometrical parameters.
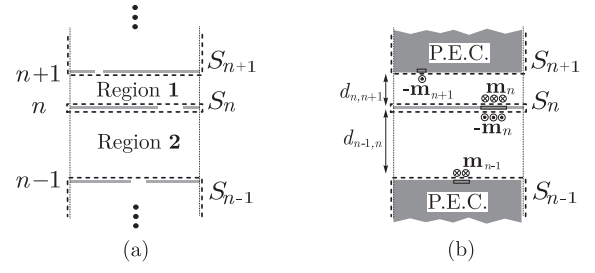

Fig. 3. (a) Original problem and (b) equivalent problem with unknown magnetic current distributions.

Fig. 4. Application of image theorem for (a) Region 1 and (b) Region 2, defined in Fig. 3.

II. z-Aperiodic Artificial Dielectric Layers

A. Problem Definition and Equivalence Principle

The geometry under consideration is shown in Fig. 2 and consists of N layers with indexes $n \in [1, 2, ..., N]$. Each layer is an array of perfectly conducting square patches, infinitely thin along z and doubly periodic in the transverse dimensions. The periods are equal along x and y and given by p. Although the transverse periods are assumed to be the same for all the layers, all other geometrical parameters can vary in each layer and they are function of the index n. The gaps between the patches in the n-th layer are characterized by width w_n both along x and y. The distance between any pair of contiguous layers, with indexes n and $n + 1$, is denoted by $d_{n,n+1}$ and can change arbitrarily along the stratification. Also the mutual shift between adjacent layers $s_{n,n+1}$ can vary with n and can be an arbitrary portion of the unit cell.

A plane wave is assumed to propagate in the negative z-direction within the ADL structure. By applying the Schelkunoff's equivalence principle [19], three surfaces S_{n+1}, S_n and S_{n-1} are defines as in Fig. 3(a) and they are filled with a perfect electric conductor (Fig. 3(b)) so that two closed regions are created. Equivalent surface magnetic currents $\mathbf{m}_n$ can be defined in correspondence of the gaps in the original problem. These current densities $\mathbf{m}_n(\boldsymbol{\rho}; w_n)$ are functions of the position $\boldsymbol{\rho} = x\hat{\mathbf{x}} + y\hat{\mathbf{y}}$ and depend on the width of the gaps w_n characteristic of the n-th layer.

Due to the image theorem, the magnetic currents radiating within parallel plate waveguides are equivalent to an infinite number of current contributions radiating in free space, as described in Fig. 4. The continuity of the transverse scattered magnetic field at the n-th layer (assumed to be located at $z = 0$) can be expressed as:

$$\sum_{i \text{ even}} \int_{-\infty}^{\infty} \int_{-\infty}^{\infty} 2\mathbf{m}_n(\boldsymbol{\rho}', w_n)\mathbf{g}(\boldsymbol{\rho} - \boldsymbol{\rho}', i\, d_{n,n+1})d\boldsymbol{\rho}' -$$

$$\sum_{i \text{ odd}} \int_{-\infty}^{\infty} \int_{-\infty}^{\infty} 2\mathbf{m}_{n+1}(\boldsymbol{\rho}'; w_{n+1})\mathbf{g}(\boldsymbol{\rho} - \boldsymbol{\rho}', i\, d_{n,n+1})d\boldsymbol{\rho}' +$$

$$\sum_{i \text{ even}} \int_{-\infty}^{\infty} \int_{-\infty}^{\infty} 2\mathbf{m}_n(\boldsymbol{\rho}'; w_n)\mathbf{g}(\boldsymbol{\rho} - \boldsymbol{\rho}', i\, d_{n-1,n})d\boldsymbol{\rho}' -$$

$$\sum_{i \text{ odd}} \int_{-\infty}^{\infty} \int_{-\infty}^{\infty} 2\mathbf{m}_{n-1}(\boldsymbol{\rho}'; w_{n-1})\mathbf{g}(\boldsymbol{\rho} - \boldsymbol{\rho}', i\, d_{n-1,n})d\boldsymbol{\rho}' = 0 \quad (1)$$

where i is the index of the spatial infinite sum of current contributions resulting from the image theorem. The observation and the source points are $\boldsymbol{\rho}$ and $\boldsymbol{\rho}'$, respectively, and $\mathbf{g}$ is the free-space dyadic Green's function, which links the magnetic field to magnetic sources. Since the structure is not periodic along z, the current densities on the layers are not related by either Floquet boundary condition or glide symmetry conditions. However, we assume here that the magnetic currents on different layers are approximately related as

$$\mathbf{m}_{n+1}(\boldsymbol{\rho}; w_{n+1}) \approx \mathbf{m}_n(\boldsymbol{\rho} - \mathbf{s}_{n,n+1}; w_{n+1}) e^{-j\psi_{n,n+1}} \quad (2)$$

$$\mathbf{m}_{n-1}(\boldsymbol{\rho}; w_{n-1}) \approx \mathbf{m}_n(\boldsymbol{\rho} - \mathbf{s}_{n-1,n}; w_{n-1}) e^{-j\psi_{n-1,n}} \quad (3)$$

where $\mathbf{s}_{n,n+1} = s_{n,n+1}\hat{\mathbf{x}} + s_{n,n+1}\hat{\mathbf{y}}$ is the vector shift along x and y and $\psi_{n,n+1}$ is a phase shift describing the propagation from one layer to the next. The conditions (2) and (3) imply that the magnetic current densities on different layers have the same longitudinal distribution along the slots, shifted in space and with a phase delay, while only the transverse distribution changes because of the different gap widths w_n. This assumption allows writing (1) only in term of a single unknown distribution $\mathbf{m}_n$. Such condition is sufficient to apply the same procedure as in [13] to find the equivalent layer reactance analytically. The method is described in detail in [11], [12] and consists of expanding the unknown magnetic current in only four entire domain basis functions, that are enough to describe the total current distribution for any generic plane-wave incidence. The basis functions have closed-form Fourier transform, thus Galerkin projection can be applied in the spectral domain, leading to a system of 4 linear equations. The properties of the chosen basis functions allow to further simplify the problem in a system of only 2 equations, leading to an analytical solution for the equivalent layer impedance.

B. Equivalent Impedance of a Layer in a Non-Periodic Sequence

By following the procedure described in the previous section, the equivalent layer impedance is derived. For the internal layers, i.e. for $n \in [2, 3, ...N - 1]$, the layer susceptance can be written as a Floquet expansion with indexes m:

$$B_n = \frac{jp}{\zeta_0 \lambda_0} \sum_{m \neq 0} \{ S_m(w_n)[f_m(d_{n,n+1}) + f_m(d_{n-1,n})] +$$
$$S_m(w_{n+1})g_m(s_{n,n+1}, d_{n,n+1}) +$$
$$S_m(w_{n-1})g_m(s_{n-1,n}, d_{n-1,n}) \} \quad (4)$$

where we introduced the functions

$$S_m(w) = \frac{\left| \mathrm{sinc}\left(\frac{\pi m w}{p}\right) \right|^2}{|m|} \quad (5)$$

$$f_m(d) = -\cot\left(\frac{-2j\pi|m|d}{p}\right) \quad (6)$$

$$g_m(s, d) = e^{j 2\pi m s/p} \csc\left(\frac{-2j\pi|m|d}{p}\right) . \quad (7)$$

In the function definition, we omitted the dependence on the period p, since it is assumed to be fixed and equal for all the layers. For the first and last layers ($n = 1$ and $n = N$), because of the absence of one of the adjacent layers, the susceptance changes as
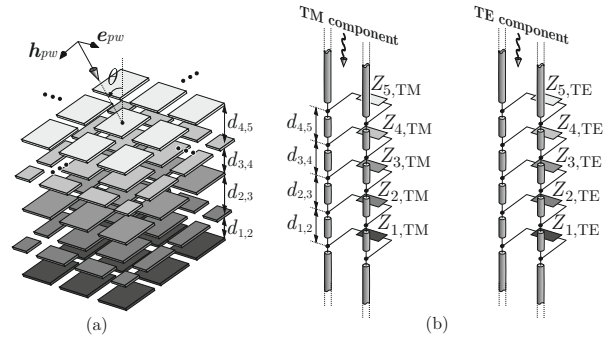

Fig. 5. (a) Plane wave incident on a structure of five ADLs with non-identical layers; (b) Equivalent circuits for TE and TM components.

$$B_1 = \frac{jp}{\zeta_0 \lambda_0} \sum_{m \neq 0} \{ S_m(w_1)[-j + f_m(d_{1,2})] +$$
$$S_m(w_2)g_m(s_{1,2}, d_{1,2}) \} \quad (8)$$

$$B_N = \frac{jp}{\zeta_0 \lambda_0} \sum_{m \neq 0} \{ S_m(w_N)[-j + f_m(d_{N-1,N})] +$$
$$S_m(w_{N-1})g_m(s_{N-1,N}, d_{N-1,N}) \} . \quad (9)$$

An equivalent transmission line circuit, similar to the one introduced in [12] and [13], can be used for the ADL with non-identical layers. The equivalent reactances of the individual layers are represented in terms of the suceptances as follows:

$$Z_{n,TM} = \frac{-j}{B_n} \quad (10)$$

and

$$Z_{n,TE} = \frac{-j}{B_n \left(1 - \frac{\sin^2(\theta)}{2} \right)} \quad (11)$$

for the TM and TE modes, respectively, where θ is the angle of incidence of an incoming plane wave.

These reactances are placed as shunt impedances along a z-oriented transmission line, which describes the propagation of a generic plane wave through the ADL. An example of a five-layer structure is shown in Fig. 5(a) and its TE and TM equivalent transmission line circuits in Fig. 5(b).

III. VALIDATION OF THE CLOSED-FORM SOLUTIONS

To validate the provided formulas, some numerical examples are considered in this section. The reflection and transmission coefficients are calculated with the analytical transmission line models and compared with CST simulations of the same structure, for TE and TM incident plane waves. All given examples assume an ADL structure consisting of five layers, with period in x- and y-direction $p = 0.0785\lambda_0$, where λ_0 is the wavelength in free space at $5\,\mathrm{GHz}$. The angle of incidence of the plane wave is $\theta = 60°$.

Figure 6 shows the S-parameters of the plane wave, when the width of the gap between the patches is varied for each
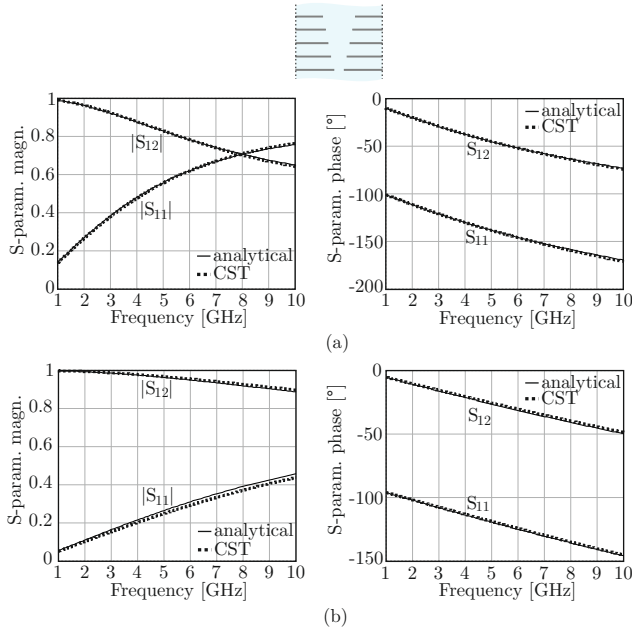
Fig. 6. Amplitude and phase of the reflection and transmission coefficients of a plane wave incident on an ADL consisting of five layers. The value of w_n is varying between the layers: $w_1 = 0.01\lambda_0$, $w_2 = 0.015\lambda_0$, $w_3 = 0.02\lambda_0$, $w_4 = 0.025\lambda_0$ and $w_5 = 0.03\lambda_0$. The other geometrical parameters are constant: $p = 0.0785\lambda_0$, $d = 0.012\lambda_0$. No shift between the layers is present. λ_0 is the wavelength in free space at 5 GHz. The angle of incidence $\theta = 60°$. (a) TE-incidence. (b) TM-incidence.

Fig. 7. Amplitude and phase of the reflection and transmission coefficients of a plane wave incident on an ADL consisting of five layers. The shift between adjacent layers is varying throughout the structure: $s_{1,2} = 0$, $s_{2,3} = 0.1p$, $s_{3,4} = 0.3p$ and $s_{4,5} = 0.4p$. The other geometrical parameters are constant: $p = 0.0785\lambda_0$, $d = 0.012\lambda_0$ and $w = 0.01\lambda_0$. λ_0 is the wavelength in free space at 5 GHz. The angle of incidence $\theta = 60°$. (a) TE-incidence. (b) TM-incidence.

layer, while all other parameters are constant. The inter-layer distance in the z-direction is $d = 0.012\lambda_0$, and no shift between the layers is present. The widths of the gaps are $w_1 = 0.01\lambda_0$, $w_2 = 0.015\lambda_0$, $w_3 = 0.02\lambda_0$, $w_4 = 0.025\lambda_0$ and $w_5 = 0.03\lambda_0$. Figure 7 shows the S-parameters for the same structure, when the width of the gaps between the patches is constant, $w = 0.01\lambda_0$, and the relative shift between adjacent layers is varying: $s_{1,2} = 0$, $s_{2,3} = 0.1p$, $s_{3,4} = 0.3p$ and $s_{4,5} = 0.4p$. Figure 8 refers to varying values of the distance between adjacent layers: $d_{1,2} = 0.01\lambda_0$, $d_{2,3} = 0.015\lambda_0$, $d_{3,4} = 0.02\lambda_0$ and $d_{4,5} = 0.025\lambda_0$. The width of the gap between the patches is constant, $w = 0.01\lambda_0$, and no relative shift between the layers is present.

In the final example, the three characteristic geometrical parameters are varied all together. The widths of the gaps are $w_1 = 0.01\lambda_0$, $w_2 = 0.015\lambda_0$, $w_3 = 0.02\lambda_0$, $w_4 = 0.025\lambda_0$ and $w_5 = 0.03\lambda_0$. The distance between the layers is growing with the indexes $d_{1,2} = 0.01\lambda_0$, $d_{2,3} = 0.015\lambda_0$, $d_{3,4} = 0.02\lambda_0$ and $d_{4,5} = 0.025\lambda_0$. The relative shift between the layers is decreasing: $s_{1,2} = 0.4p$, $s_{2,3} = 0.3p$, $s_{3,4} = 0.1p$ and $s_{4,5} = 0$. The resulting reflection and transmission coefficients are shown in Fig. 9 for TE- and TM-incidence.

In all presented results a good agreement between the analytical formulas and CST is observed.

IV. CONCLUSION

We presented analytical formulas for the analysis of non-periodic ADLs. Closed-form expressions for the equivalent
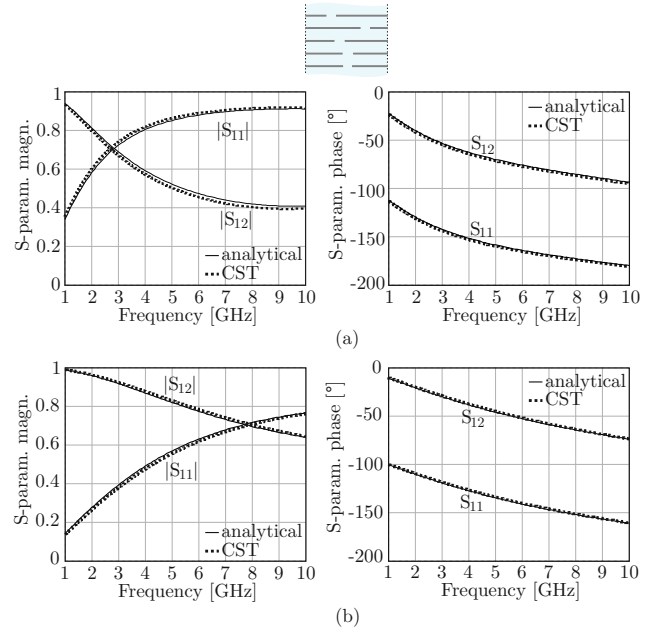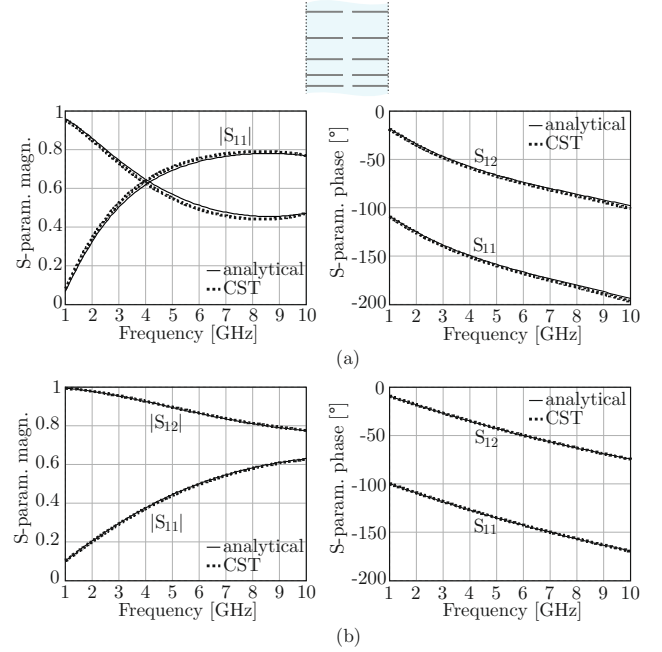

Fig. 8. Amplitude and phase of the reflection and transmission coefficients of a plane wave incident on an ADL consisting of five layers. The distance in z-direction between adjacent layers is varying throughout the structure: $d_{1,2} = 0.01\lambda_0$, $d_{2,3} = 0.015\lambda_0$, $d_{3,4} = 0.02\lambda_0$ and $d_{4,5} = 0.025\lambda_0$. The other geometrical parameters are constant: $p = 0.0785\lambda_0$ and $w = 0.01\lambda_0$. No shift between the layers is present. λ_0 is the wavelength in free space at 5 GHz. The angle of incidence $\theta = 60°$. (a) TE-incidence. (b) TM-incidence.
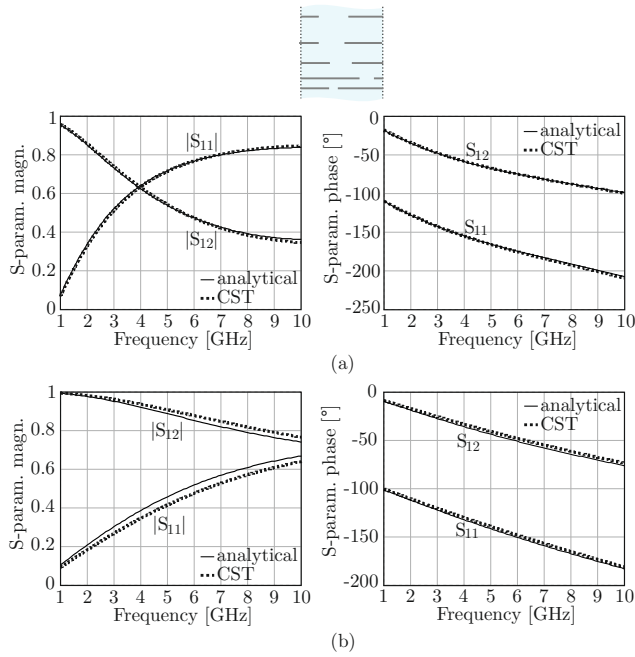
Fig. 9. Amplitude and phase of the reflection and transmission coefficients of a plane wave incident on an ADL consisting of five layers. The period in x and y is $p = 0.0785\lambda_0$. The other geometrical parameters are changing throughout the structure: $w_1 = 0.01\lambda_0$, $w_2 = 0.015\lambda_0$, $w_3 = 0.02\lambda_0$, $w_4 = 0.025\lambda_0$ and $w_5 = 0.03\lambda_0$, $s_{1,2} = 0$, $s_{2,3} = 0.1p$, $s_{3,4} = 0.3p$ and $s_{4,5} = 0.4p$, and $d_{1,2} = 0.01\lambda_0$, $d_{2,3} = 0.015\lambda_0$, $d_{3,4} = 0.02\lambda_0$ and $d_{4,5} = 0.025\lambda_0$. λ_0 is the wavelength in free space at $5\,\mathrm{GHz}$. The angle of incidence $\theta = 60°$. (a) TE-incidence. (b) TM-incidence.

layer impedance for generic plane wave incidence were derived. The proposed formulas are more general than those presented in previous works. The individual layers may be different from each other in terms of geometrical parameters and the mutual distance and shift between adjacent layers may vary along the stratification. Results from the analytical formulas were validated by comparison with a commercial electromagnetic solver. By dropping the restriction of identical layers, the expressions can be used to design ADLs that are not uniform along the vertical dimension. Possible applications can be tapered impedance transformers to realize wideband matching slabs or wide angle impedance matching superstrates for broadband phased arrays.

REFERENCES

[1] W. E. Kock, "Metallic delay lenses," *Bell System Tech. J.*, vol. 27, no. 1, pp. 58-82, Jan. 1948.

[2] S. S. D. Jones and J. Brown, "Metallic delay lenses," *Nature*, vol. 163, no. 4139, pp. 324-325, Feb. 1949.

[3] R. E. Collin, *Field Thery of Guided Waves, 2nd Ed.* IEEE Press, New York, 1990.

[4] D. Cavallo, W. H. Syed and A. Neto, "Artificial dielectric enabled antennas for high frequency radiation from integrated circuits," *11th Eur. Conf. Antennas Propagation*, Paris, 2017, pp. 1626-1628.

[5] W. H. Syed, G. Fiorentino, D. Cavallo, M. Spirito, P. M. Sarro, and A. Neto, "Design, fabrication and measurement of 0.3 THz on-chip double-slot antenna enhanced by artificial dielectrics," *IEEE Trans. THz Sci. Tech.*, vol. 5, no. 2, pp. 288-298, Mar. 2015.

[6] W. H. Syed, D. Cavallo, H. Thippur Shivamurthy, and A. Neto, "Wide-band, wide-scan planar array of connected slots loaded with artificial dielectric superstrates," *IEEE Trans. Antennas Propag.*, vol. 64, no. 2, pp. 543-553, Feb. 2016.

[7] D. Cavallo, W.H. Syed, and A. Neto, "Connected-slot array with artificial dielectrics: A 6 to 15 GHz dual-pol wide-scan prototype," *IEEE Trans. Antennas Propag.*, vol. 66, no. 6, pp. 3201-3206, Jun. 2018.

[8] E. Martini, G. M. Sardi and S. Maci, "Homogenization processes and retrieval of equivalent constitutive parameters for multisurface-metamaterials," *IEEE Trans. Antennas Propag.*, vol. 62, no. 4, pp. 2081-2092, April 2014.

[9] S. Barzegar-Parizi and B. Rejaei, "Calculation of effective parameters of high permittivity integrated artificial dielectrics," *IET Microwaves, Antennas Propag.*, vol. 9, no. 12, pp. 1287-1296, Sep. 2015.

[10] F. Mesa, R. Rodrguez-Berral, M. Garca-Vigueras, F. Medina and J. R. Mosig, "Simplified modal expansion to analyze frequency-selective surfaces: An equivalent circuit approach," *IEEE Trans. Antennas Propag.*, vol. 64, no. 3, pp. 1106-1111, March 2016.

[11] D. Cavallo, W. H. Syed, and A. Neto, "Closed-form analysis of artificial dielectric layers−Part I: Properties of a single layer under plane-wave incidence," *IEEE Trans. Antennas Propag.*, vol. 62, no. 12, pp. 6256-6264, Dec. 2014.

[12] D. Cavallo, W. H. Syed, and A. Neto, "Closed-form analysis of artificial dielectric layers−Part II: Extension to multiple layers and arbitrary illumination," *IEEE Trans. Antennas Propag.*, vol. 62, no. 12, pp. 6265-6273, Dec. 2014.

[13] D. Cavallo and C. Felita, "Analytical formulas for artificial dielectrics with nonaligned layers," *IEEE Transactions on Antennas and Propagation*, vol. 65, no. 10, pp. 5303-5311, Oct. 2017.

[14] D. Cavallo, "Dissipation losses in artificial dielectric layers," *IEEE Transactions on Antennas and Propagation*, vol. 66, no. 12, 2018.

[15] G. Valerio, Z. Sipus, A. Grbic, and O. Quevedo-Teruel, "Accurate equivalent-circuit descriptions of thin glide-symmetric corrugated meta-surfaces," *IEEE Trans. Antennas Propag.*, vol. 65, no. 5, pp. 2695-2700, May 2017.

[16] J. R. Wait, "Theories of scattering from wire-grid and mesh structures," in *Electromagnetic Scattering*, P.L.E. Uslenghi, Ed. New York: Academic, 1978, pp. 253-287.

[17] R. C. Compton and D. B. Rutledge, "Approximation techniques for planar periodic structures," *IEEE Trans. Microw. Theory Techniques*, vol. 33, no. 10, pp. 1083-1088, Oct. 1985.

[18] O. Luukkonen, C. Simovski, G. Granet, G. Goussetis, D. Lioubtchenko, A. V. Raisanen, and S. A. Tretyakov, "Simple and accurate analytical model of planar grids and high-impedance surfaces comprising metal strips or patches," *IEEE Trans. Antennas Propag.*, vol. 56, no. 6, pp. 1624-1631, Jun. 2008.

[19] S. A. Schelkunoff, "Some equivalence theorems of electromagnetics and their application to radiation problems," *Bell System Tech. J.*, vol. 15, pp. 92112, 1936.